

# Characterization of Seismic Newtonian Noise

Author: Alexander Hipp

*Edgewood College*

Mentors: Dr. Ik Siong Heng

*Institute for Gravitational Research, University of Glasgow*

Daniel Williams

*Institute for Gravitational Research, University of Glasgow*

July 31, 2018

## Abstract

In this paper we present the first steps of a project to develop a model that can take seismic measurements from the gravitational wave detector sites, predict the seismic field around the test mass, and calculate the seismic Newtonian noise. We developed several models that simulate seismic fields and can calculate the seismic Newtonian noise from them, as well as an initial Gaussian Process regression model that is trained on data from our one-dimensional model. The models built are capable of simulating seismic fields with varying degrees of complexity, with one model close to simulating actual environments. The first results of the Gaussian Process regression model were accurate and provide motivation for improvement. The models completed thus far are a positive first step in the completion of this project.

## 1 Introduction

In 1915 Albert Einstein published his Theory of General Relativity, which predicts the existence of gravitational waves. These waves are produced by the acceleration of massive objects, propagate at the speed of light, and stretch and compress the fabric of spacetime in orthogonal directions. The

current method for detecting gravitational waves is the utilization of an advanced, massive Michelson interferometer, as used by LIGO, Virgo, and other observatories. Past detections have shown that the strength of gravitational wave signals once they reach Earth is remarkably weak, with the first detection GW150914 having a strain of  $10^{-21}$ . This presents a major challenge in successfully detecting gravitational waves, as there are numerous sources of noise in the detectors that can cause the signal to become undetectable. Shown below is the Advanced Virgo sensitivity curve.

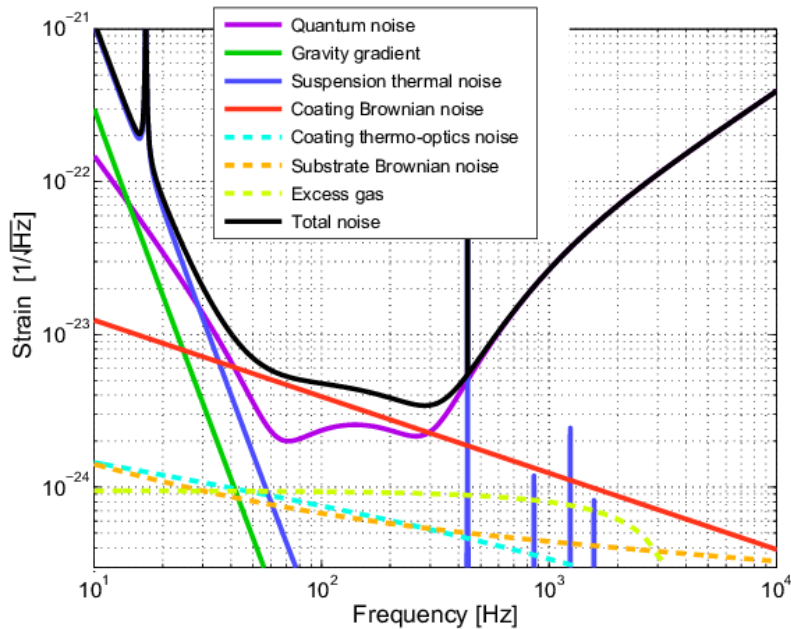


Figure 1: This is the Advanced Virgo Sensitivity curve and shows the strength of each source of noise in an equivalent gravitational wave amplitude.

As shown in this graph, the strength of the noise signals increase at lower

frequencies, making gravitational waves with signals below approximately 10Hz quite difficult to detect. The noise source that this paper is concerned with is the gravity gradient noise, or Newtonian noise. Newtonian noise results from the acceleration of the test mass due to fluctuations in the gravitational field surrounding it. At low frequencies, Newtonian noise becomes one of the dominant sources of noise and must be mitigated if we hope to detect gravitational wave signals at low frequencies. There are many sources of Newtonian noise, however they can be divided into three categories: seismic, atmospheric, anthropogenic [1]. In this paper, we explore the seismic contributions to Newtonian noise. The goal of this project is to develop a model that takes a small amount of seismic measurements from the field surrounding the test mass and predicts the entire field, then calculates the Newtonian noise from that field. In the following sections, we will present various models to calculate the Newtonian noise from seismic fields and present a Gaussian Process Regression model to make predictions of the Newtonian noise.

## 2 Background

### 2.1 Seismic Waves

The source of seismic Newtonian noise is seismic waves passing through the medium surrounding the test mass. The three types of seismic waves are shear waves or S-waves, compressional waves or P-waves, and surface waves. Shear waves are transverse waves and displace the medium perpendicular to its direction of propagation thus they have two polarizations, the horizontal

polarization is parallel to the surface and the vertical polarization is perpendicular to the surface. Compressional waves are longitudinal waves and compress and expand the medium in the direction of propagation. The main type of surface wave is the Rayleigh wave, which both compresses and expands the medium and displaces the medium perpendicular to the surface. Rayleigh waves can be decomposed into P-wave and vertically polarized S-wave components. Figure 2 below provides a representation of each type of wave, including love waves which we are not concerned with in our study of seismic Newtonian noise.

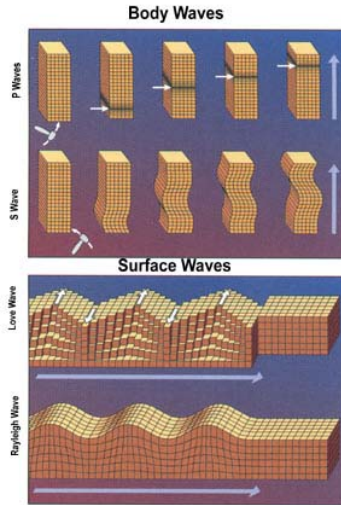


Figure 2: Representatin of P-waves, S-waves, Rayleigh waves, and Love waves.

The amplitude of Rayleigh waves is significantly larger than the other waves[1] and thus will be our focus. We define  $k_\rho$  to be the horizontal wavenumber,  $k_P$  is the wavenumber of the P-wave contribution, and  $k_S$  is the wavenumber of the S-wave. Similarly, we define  $\vec{k}_\rho$  be the horizontal

wave vector and  $\vec{k}_z$  be the vertical wave vector. The vertical and horizontal amplitudes of the Rayleigh wave are given by:

$$\begin{aligned}\xi_k(\vec{r}, t) &= A \cdot (k_\rho e^{q_z^P z} - \zeta q_z^S e^{q_z^S z}) \cdot \sin(\vec{k}_\rho \cdot \vec{\rho} - \omega t) \\ \xi_z(\vec{r}, t) &= A \cdot (q_z^P e^{q_z^P z} - \zeta k_\rho e^{q_z^S z}) \cdot \cos(\vec{k}_\rho \cdot \vec{\rho} - \omega t)\end{aligned}\quad (1)$$

Where the variables  $q_z^P$ ,  $q_z^S$ , and  $\zeta$  are wave paramaters given by:

$$\begin{aligned}q_z^P &= \sqrt{k_\rho^2 - (k^P)^2} \\ q_z^S &= \sqrt{k_\rho^2 - (k^S)^2} \\ \zeta(k_\rho) &= \sqrt{\frac{q_z^P}{q_z^S}}\end{aligned}\quad (2)$$

The displacement of Rayleigh waves, although surface waves, do extend evanescently through the medium. Using the wave paramters above, the difference between the exponentials in equation 1 describes how exactly this occurs. Defining  $C_R$  be the speed of the Rayleigh and  $C_S$  to be speed of S-wave component, the ratio  $\frac{C_R^2}{C_S^2}$  obeys the equations:

$$\left(\frac{C_R^2}{C_S^2}\right)^3 - 8\left(\frac{C_R^2}{C_S^2}\right)^2 + 8\left(\frac{C_R^2}{C_S^2}\right)\frac{2-\nu}{1-\nu} - \frac{8}{1-\nu} = 0 \quad (3)$$

The variable  $\nu$  is Poisson's ratio is a property of the medium. Finally, the seismic displacement vector is given by:

$$\xi(\vec{r}, t) = \xi_k(\vec{r}, t)\vec{e}_k + \xi_z(\vec{r}, t)\vec{e}_z \quad (4)$$

The vector  $\vec{e}_k$  is the unit vector in the direction of the Horizontal wave vector which is also the direction of propagation of the wave and the vector

$\vec{e}_z$  is the unit vector in the direction of the z-axis. A detailed derivation of the equations above can be found in Jan Harm’s paper ”Terrestrial Gravity Fluctuations” [?]. Using these equations we are able to determine the seismic displacement field and how it changes with time and position.

## 2.2 Seismic Newtonian Noise

As seismic waves pass through the medium around the test mass, they cause density fluctuations in the medium and produces the seismic Newtonian noise. In our model, we consider a Rayleigh wave passing through a homogeneous half-medium, as shown in the figure below.

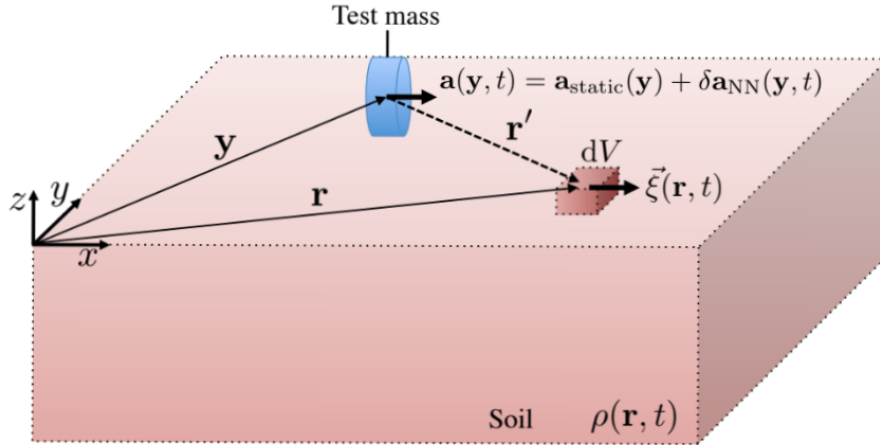


Figure 3: This figure, taken from Beker’s paper ”Low-frequency sensitivity of next generation gravitational wave detectors” [2], show the homogeneous half-medium and coordinate system used in our model.

The total seismic Newtonian noise is due to the density fluctuations caused by the Rayleigh wave in the medium and at the boundary. The contributions of each are given by:

$$\begin{aligned}\delta\vec{a}_{NN}, Med(\vec{y}, t) &= G\rho_0 \int_V (\vec{\xi}(\vec{r}, t) \cdot \nabla) \vec{k} dV - G\rho_0 \int_S (\vec{\xi}(\vec{r}, t) \cdot \hat{n}(\vec{r})) \vec{k} dS \\ \delta\vec{a}_{NN}, Bound(\vec{y}, t) &= G\rho_0 \int_S (\vec{\xi}(\vec{r}, t) \cdot \hat{n}(\vec{r})) \vec{k} dS\end{aligned}\quad (5)$$

Where the vector  $\vec{k}$  is defined as:

$$\vec{k} = \frac{\vec{r}'}{|\vec{r}'|^3} \quad (6)$$

Taking the sum of these contributions gives the total seismic Newtonian noise:

$$\delta\vec{a}_{NN}(\vec{y}, t) = G\rho_0 \int_V (\vec{\xi}(\vec{r}, t) \cdot \nabla) \vec{k} dV \quad (7)$$

A formal derivation of these equations can be found in Beker's paper "Low-frequency sensitivity of next generation gravitational wave detectors" [2]. In this paper, Beker also derives an equation for the total seismic Newtonian noise for numerical analysis from the equation above, given by:

$$\delta\vec{a}_{NN}(\vec{y}, t) = G\rho_0 \sum i^N \frac{1}{|\vec{r}'_i|^3} (\vec{\xi} - 3(\vec{\xi} \cdot \hat{r}'_i) \hat{r}'_i) \cdot V_i \quad (8)$$

With  $\hat{r}'_i$  defined as the unit vector that points from the test mass to the  $i$ th volume element. Using this equation, along with equations 4 and 1 a finite element model to calculate the seismic Newtonian noise can be built.

## 2.3 Gaussian Processes

Gaussian Processes are powerful tools, particularly in regression modeling. One way to think of a Gaussian Process regression model is as distribution of functions. Suppose we have a collection of observations  $(y_1, y_2, \dots, y_n)$  that follow a normal distribution at locations  $(x_1, x_2, \dots, x_n)$  in some parameter space, where  $y = f(x)$ . We define a covariance matrix  $\Sigma$ , this must take a specific form however we will not provide detail regarding that, for  $(x_i, x_j)$  for every pair of parameters where an observation was made and a mean function  $\mu$ . These form a Gaussian process prior, from which we make predictions and form a posterior distribution. This posterior distribution, rather than providing one fit it produces many functions to fit the data, so the posterior distribution is as mentioned before a distribution of functions. The significance of the Gaussian Process regression model is it produces many functions and provides information for how good the mean function it outputs is. Shown below is an example of a Gaussian Process regression model.

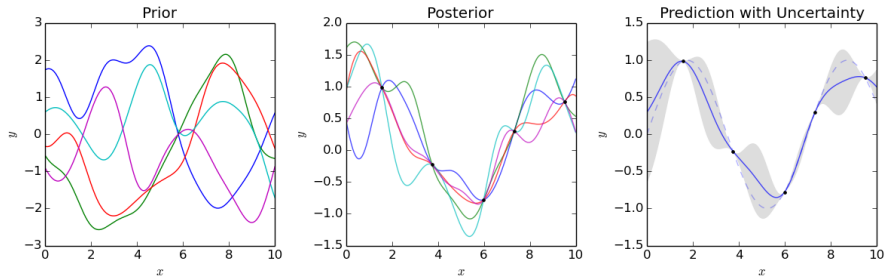


Figure 4: The prior, posterior, and posterior with uncertainty of a Gaussian Process regression model.

## 3 Results

### 3.1 Single Wave Models

The single wave models were the simplest implementations of equations 1, 4, and 8. We built an one-dimensional, two-dimensional, and three-dimensional model<sup>1</sup> in which the seismic field is produced by a Rayleigh wave with known parameters. The wave parameters defined in equation 2 are determined by knowing the speed of the Rayleigh wave, the P-wave component, and the S-wave component and the direction of propagation. A method for determining the speed of the various components is presented in Beker's paper. First, we determined the speed of the P-wave component using the equation:

$$\rho = \alpha C_P^\beta \quad (9)$$

Where  $\rho$  is the density of the medium and  $\alpha$  and  $\beta$  are parameters. They suggest setting  $\alpha = 0.31$  and  $\beta = 0.25$  for accurate predictions for the range of density values used for Virgo, which we did. Next, we used the P-wave speed,  $C_P$  to determine the speed of the S-wave component using the following relationship:

$$\frac{C_S}{C_P} = \sqrt{\frac{1 - 2\nu}{2 - 2\nu}} \quad (10)$$

We then used  $C_S$  and equation 3 to determine the speed of the Rayleigh wave,  $C_R$ . Once these speeds were determined and a direction of propaga-

---

<sup>1</sup>We built all models in Python using the Python packages Numpy, Matplotlib, and Itertools.

tion was chosen, the remaining parameters could be calculated. The main parameters of our model that we changed were  $\alpha$ ,  $\beta$ ,  $\nu$ , and  $\rho$  as all other parameters are determined by knowing these values. Using these parameters we defined the seismic displacements using equation 1, where our inputs were the x, y, and z positions, the time, frequency, angle of propagation relative to the x-axis, and we added a phase shift. Lastly, we also defined two equations using equation 8. The first was to calculate the contribution of a single point in the field at a given time and the second was to calculate the total seismic Newtonian noise due to the entire field at a given point in time. The differences between the different dimensional models are minimal, for example the one-dimensional did not include a direction of propagation as the wave was set to travel along the x-axis, so the propagation angle was left out. Below are results obtained from these models.

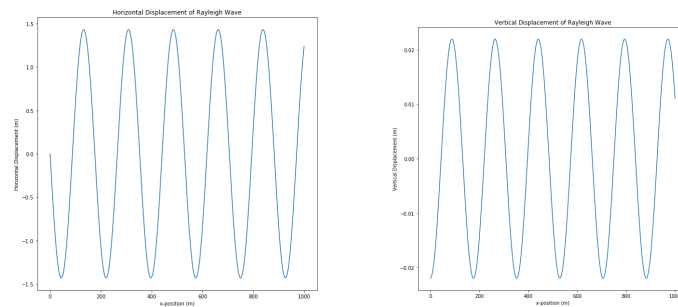


Figure 5: The horizontal and vertical seismic displacements for a Rayleigh wave with a speed of 350m/s and a frequency of 2Hz from the one-dimensional model.

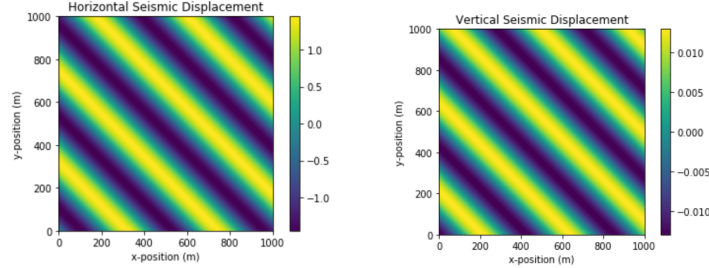


Figure 6: The horizontal and vertical seismic displacements for a Rayleigh wave with a speed of 1136m/s, an angle of propagation of  $45^\circ$ , and a frequency of 2Hz from the one-dimensional model.

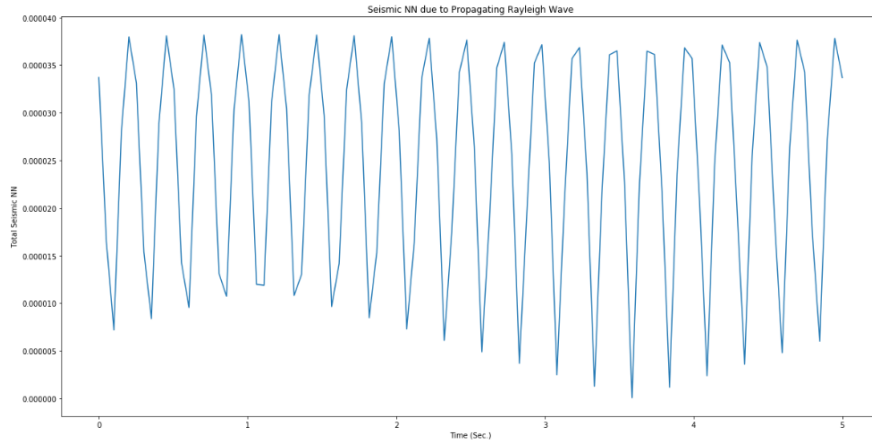


Figure 7: This is the time series of the seismic Newtonian noise produced by a Rayleigh wave with a speed of 1136m/s, an angle of propagation of  $45^\circ$ , and a frequency of 2Hz from the three-dimensional model. This was calculated using a grid of 500m  $\times$  500m grid centered on the test mass, with a depth of 100m. The points in the grid were equally spaced with dimensions  $101 \times 101 \times 11$ .

### 3.2 Multi Wave Models

The multi-wave models we developed are extensions of the models discussed in the previous section. We decided to build a two-dimensional and three

dimensional multi-wave model. We defined the parameters in these models exactly the same as we did in the single-wave models. The main difference in moving to these models is that the seismic field is now the superposition of five Rayleigh waves with frequencies 2Hz, 4Hz, 6Hz, 8Hz, and 10Hz. We also included a frequency dependent amplitude for amplitude of the displacements for each wave. To determine the function for this frequency dependent amplitude we began with the Rayleigh wave spectral density graph shown below:

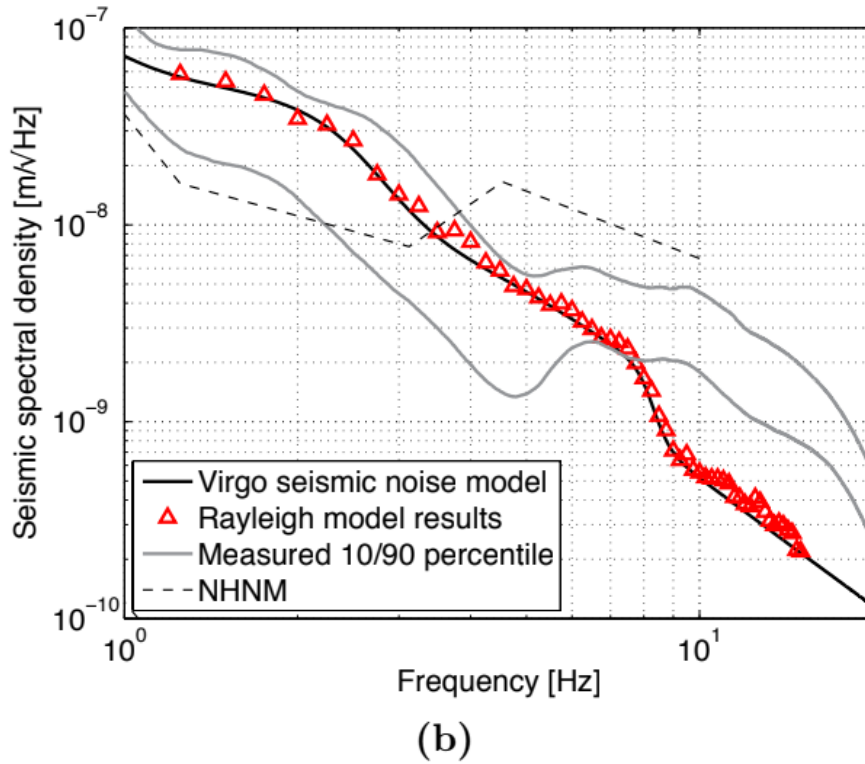


Figure 8: The amplitude spectral density graph for Rayleigh waves [2]

We used a simple approach of estimating a line that passes through the

points  $(2, 4 \cdot 10^{-8})$  and  $(10, 5 \cdot 10^{-8})$ . From this, we were able to find determine the equation to be:

$$A(f) = \frac{4 \cdot 10^{-8}}{2^{-2.72}} \cdot f^{-2.72} \quad (11)$$

We then rescaled it so that  $A(2) = 1$ , giving us:

$$A(f) = \frac{1}{2^{-2.72}} \cdot f^{-2.72} \quad (12)$$

We assigned to each frequency a phase shift and angle of propagation as well to make interpreting the results more straightforward. However, we did include equations where the phase shift and direction of propagation for each wave were normal distributed random variables. Below are some results obtained from this model.

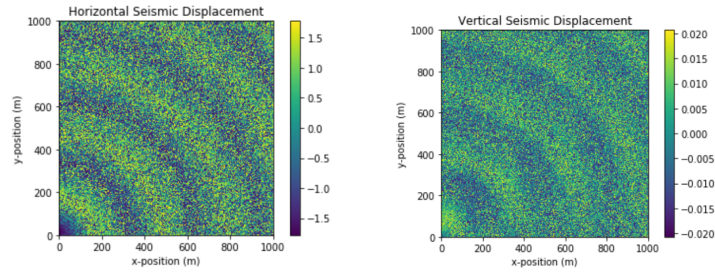


Figure 9: The horizontal and vertical seismic displacements for a superposition of Rayleigh waves with a speed of 1136m/s from the two-dimensional model.

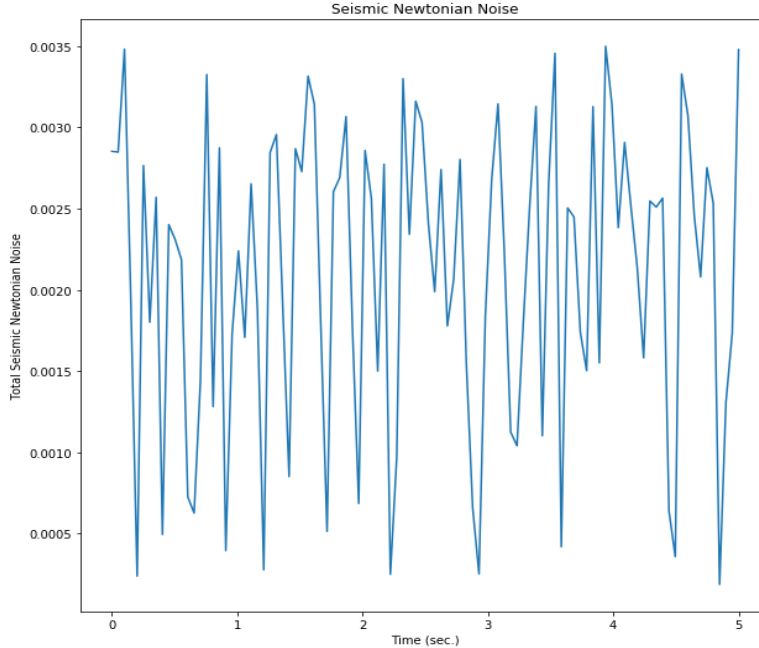


Figure 10: This is the time series of the seismic Newtonian noise from the superposition of the five Rayleigh waves with a speed of 1136m/s. The grid used for the calculation was a  $500\text{m} \times 500\text{m}$  centered on the test mass and the points calculated at were equally spaced through this grid with dimensions  $31 \times 31 \times 7$ .

### 3.3 Gaussian Process Regression

For the Gaussian Process regression model, we used the one-dimension model from section 3.1 and added the frequency dependent amplitude to it. Our approach for the Gaussian Process regression model was to use as few seismic displacement observations as possible such that we could accurately predict the remainder of the field surrounding the test mass and calculate the seismic Newtonian noise. We built two Gaussian Process regression model, one to make predictions for the horizontal seismic displacements and to make

predictions for the vertical seismic displacements. For our model<sup>2</sup>, we used the Pymc3 Marginal likelihood implementation for regression. With this, we used the default mean function which is the zero mean and for the covariance function we used the exponentiated quadratic. We added a miniscule amount of noise following a normal distribution as a prior to increase numerical stability. The other prior added was for the length scale of the covariance function, which we defined as to be drawn from a normal distribution with mean 120 and standard deviation 20. Shown below are a few predictions made by the model.

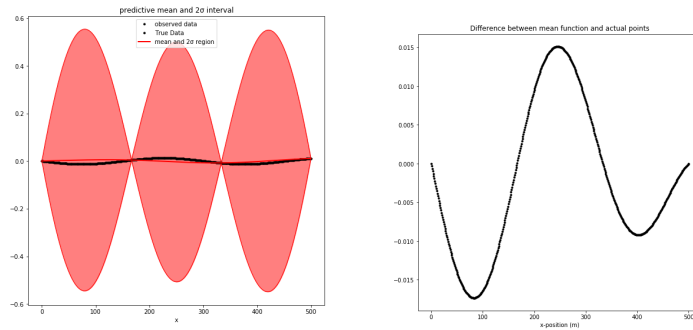


Figure 11: This is the prediction after training the model for the vertical displacements on 4 points equally spaced between 0m and 500m for a Rayleigh wave with a speed of 1136m/s and a frequency of 2Hz, along with a graph showing the difference between the mean function and the actual values.

<sup>2</sup>We built our model using the Numpy, Matplotlib, itertools, and Pymc3 packages in Python, leaning heavily on the Gaussian Process tools in the Pymc3 package.

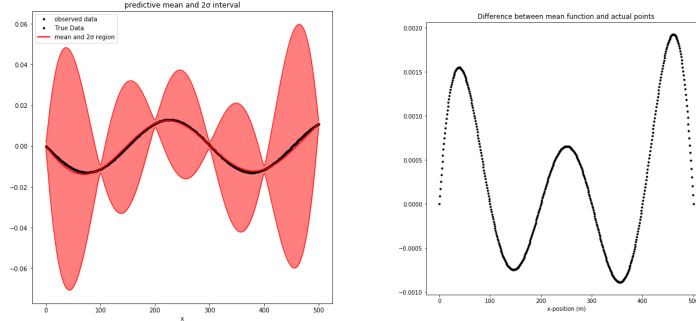


Figure 12: This is the prediction after training the model for the vertical displacements on 6 points equally spaced between 0m and 500m for a Rayleigh wave with a speed of 1136m/s and a frequency of 2Hz, along with a graph showing the difference between the mean function and the actual values.

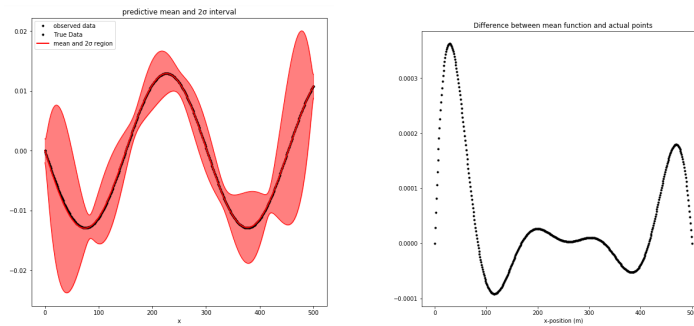


Figure 13: This is the prediction after training the model for the vertical displacements on 7 points equally spaced between 0m and 500m for a Rayleigh wave with a speed of 1136m/s and a frequency of 2Hz, along with a graph showing the difference between the mean function and the actual values .

From these outputs we can see that training the model on just seven observations results in a mean function that is very close to the actual data, the model trained on six observations does quite well too, however once we get down to training the model on four observations the mean function is clearly wrong. This pattern of results held for the horizontal model as well. We proceeded to use the models to make predictions for an entire times

series, training the models on seven points for each time step and used these predictions to produce a prediction of the time series of the seismic Newtonian noise. The results are shown below.

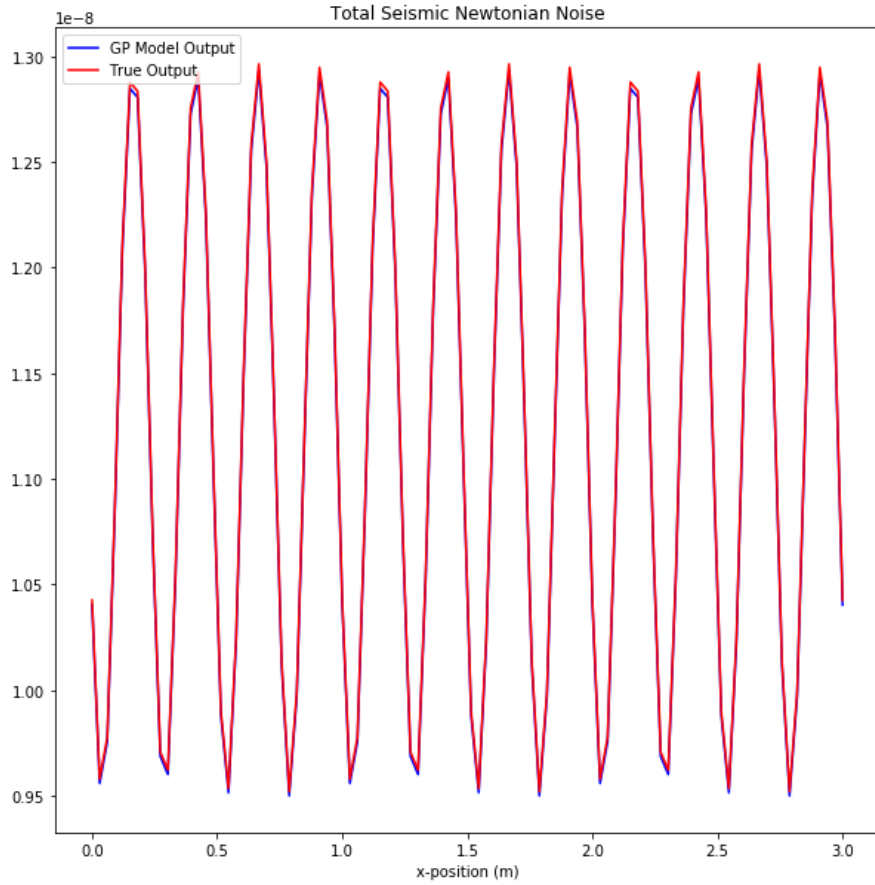


Figure 14: This shows the comparison between the time series for seismic Newtonian noise as predicted by the Gaussian Process regression model and the actual time series of the seismic Newtonian noise.

This result is was better than expected for this initial model. The model performing well after being trained on only seven observations is significant, since the Virgo detector currently uses an array of seven seismometers to

measure the seismic field at the site [2].

## 4 Conclusion

Overall, this project was successful in developing increasingly complex models to calculate the seismic Newtonian noise from seismic fields. The three-dimensional multi-wave model as discussed in section 3.2 can quite easily be made to calculate the superposition of a large number waves with varying parameters, thus making it possible to simulate quite complex seismic fields. The initial Gaussian Process regression model also had promising results. Although it was for the simplest case, having the model make quite accurate predictions after being trained on a number of observations close to the number of seismometers each observation site has demonstrates that this model adequate enough to motivate improvement. Future work will include improvements to the models discussed in sections 3.1 and 3.2 and to begin building Gaussian Process regression models that is able be trained on data from other the models developed and go towards being able to make accurate predictions for seismic Newtonian noise from predicting increasingly complex seismic fields. This results presented in this paper are a valuable first step in achieving a more developed model.

## 5 Acknowledgements

First, I would like to thank Dr. Ik Siong Heng and Daniel Williams for providing me their time and support to help complete this project, it is very

well appreciated. I would also like to thank Dr. Mueller and Dr. Whiting for their support as the program leaders. Lastly, I would like to thank the National Science Foundation for providing the funding for the IREU and making program possible.

## References

- [1] Stefan Ballmer and Vuk Mandic. *New Technologies in Gravitational-Wave Detection*. Annu. Rev. Nucl. Part. Sci. 2015. 65:555–77.
- [2] Mark Beker. *Low-frequency sensitivity of next generation gravitational wave detectors*.
- [3] Jan Harms. *Terrestrial Gravity Fluctuations*. Living Reviews In Relativity, 18(3), 1-150. doi:10.1007/lrr-2015-3.
- [4] Daniel Williams. *A Gaussian Process Tutorial*.